Validating Terrestrial SER in 12-, 28-, and 65-nm SRAMs Estimated by Simulation Coupled With One-Time Neutron Irradiation

Kazusa Takami, *Graduate Student Member, IEEE*, Yuibi Gomi, Ryuichi Yasuda, Shin-Ichiro Abe, Masatoshi Itoh, Hiroki Kanda, Mitsuhiro Fukuda, and Masanori Hashimoto, *Senior Member, IEEE*

***Abstract*— This article validates the terrestrial soft error rate (SER) estimation method proposed by Abe et al. using 12-nm FinFET and 28- and 65-nm planar static random access memories (SRAMs). Experimental results demonstrate that the SERs estimated through simulations coupled with one-time monoenergetic neutron irradiation are consistent with the SERs measured using a white neutron beam at the Research Center for Nuclear Physics (RCNP) within 70% error at the nominal operation voltage of 1.0 V for 65-nm SRAMs. In addition, the difference between the experimental results and the estimated SERs is up to 28% error for 12- and 28-nm SRAMs. Furthermore, we investigate the influence of the dielectric materials in metal layers. Although they change the energy dependence of single-event upset (SEU) cross sections, they do not significantly affect the precision of SER estimation.**

***Index Terms*— Neutrons, particle and heavy-ion transport code system (PHITS), single-event upsets (SEUs), soft error rates (SERs), soft errors.**

I. Introduction

NEUTRON-INDUCED soft errors in the terrestrial environment pose reliability issues for semiconductor devices. Evaluating the soft error rates (SERs) is crucial to ensuring the reliability of these devices. JESD89B [1] is one of the standards for SER testing.

The JESD89B standard lists several methods for estimating terrestrial SERs. The first method involves the use of white neutron sources, which can provide neutrons with spectra that closely resemble those found in the terrestrial environment. However, such sources are scarce, limiting the availability of sufficient beam time. Additionally, discrepancies in the neutron energy spectra between the ground environment and the beam facility can introduce errors in SER estimation [2], [3], [4], [5]. The second method involves deriving a Weibull function from experimental results obtained with several different beams to determine four unknown parameters. The Weibull function is expressed as

$$\sigma(E) = \sigma_{L_i}\left(1 - e^{-\left[\frac{E-E_{0i}}{W_i}\right]^{S_i}}\right) \tag{1}$$

where σ_{L_i}, E_{0i}, W_i, and S_i are unknown parameters and $\sigma(E)$ represents the single-event upset (SEU) cross section as a function of E. Then, the SER is calculated by folding the Weibull function and the flux spectrum as follows:

$$\text{SER} = \int \phi(E) \cdot \sigma(E)\, dE \tag{2}$$

where $\phi(E)$ is the differential flux of particles as a function of E.

Abe et al. [6] proposed a new method for estimating terrestrial SERs. This method derives the terrestrial SER using a one-time irradiation test with an arbitrary neutron source, coupled with Monte Carlo simulations by tools such as the particle and heavy-ion transport code system (PHITS) [7] and Geant4 [8]. They estimated the terrestrial SER for a 65-nm bulk static random access memories (SRAM) under various conditions and facilities, confirming that the ratio between the minimum and maximum estimated terrestrial SERs was 1.8. However, as there is no experimental result at white neutron sources in [6], the verification of the SER estimation method in [6] is not enough. Moreover, with the ongoing progression of process shrinkage and the increasing adoption of devices fabricated with newer processes, there is a growing demand for further experimental validation of the terrestrial SER estimation method for these advanced processes.

This work applies the terrestrial SER estimation method from [6] to 12-nm 1-fin FinFETs and 28-nm planar SRAMs, utilizing both monoenergetic and quasimonoenergetic neutron sources. We calculate the terrestrial SER using three approaches: 1) a white neutron source at the Research Center for Nuclear Physics (RCNP), serving as a reference; 2) a Weibull function for comparative analysis; and 3) the evaluation method of [6]. We then discuss the differences between these estimation methods. In addition, we conducted an irradiation experiment on the 65-nm SRAM using the spallation neutron source at the RCNP at Osaka University [9],

Received 13 September 2024; revised 28 November 2024 and 15 January 2025; accepted 22 January 2025. Date of publication 27 January 2025; date of current version 18 August 2025. This work was supported by the Grant-in-Aid for Scientific Research (S) from Japan Society for the Promotion of Science (JSPS) under Grant JP19H05664 and Grant 24H00073. *(Corresponding author: Masanori Hashimoto.)*

Kazusa Takami, Yuibi Gomi, Ryuichi Yasuda, and Masanori Hashimoto are with the Department of Informatics, Kyoto University, Kyoto 606-8501, Japan (e-mail: hashitomo@i.kyoto-u.ac.jp).

Shin-Ichiro Abe is with Japan Atomic Energy Agency (JAEA), Tōkai 319-1195, Japan.

Masatoshi Itoh is with the Research Center for Accelerator and Radioisotope Science (RARIS), Tohoku University, Sendai 980-8578, Japan.

Hiroki Kanda and Mitsuhiro Fukuda are with the Research Center for Nuclear Physics (RCNP), Osaka University, Ibaraki 567-0047, Japan.

Color versions of one or more figures in this article are available at https://doi.org/10.1109/TNS.2025.3534564.

Digital Object Identifier 10.1109/TNS.2025.3534564

evaluated the terrestrial SER, and compared with the estimated SERs reported in [6].

The remainder of this article is organized as follows. Section II outlines the SER estimation method from [6]. In Section III, the setup for simulations and experiments related to SER estimation is explained. Section IV presents the experimental results and discusses the differences between the SER estimation method in [6] and existing methods. In Section V, the influence of dielectric materials in metal layers is investigated. Finally, Section VI concludes with a brief summary.

II. Terrestrial SER Estimation Using Simulations Coupled With One-Time Neutron Irradiation

We outline the procedure of the terrestrial SER estimation method described in [6].

1) *Experiment:* Do the experiment using an unprescribed neutron source and obtain the number of SEUs $N_{\mathrm{SEU,exp}}$. The test duration t_{exp} is also required.
2) *Simulation:* Reproduce device under test (DUT) boards roughly in the simulation environment and run the Monte Carlo simulation to obtain the SEU cross section $\sigma_{\mathrm{SEU}}(E_n, Q_{\mathrm{fit}})$ as a function of neutron energy E_n and Q_{fit}. Q_{fit} represents the charge amount necessary to cause SEUs, and it is used as a calibration parameter between simulation and measurement.
3) *Decision on Q_{fit}:* Determine the value of Q_{fit} in order that the number of SEUs in simulation $N_{\mathrm{SEU,calc}}(Q_{\mathrm{fit}})$ corresponds to that in the experiment $N_{\mathrm{SEU,exp}}$. The number of SEUs in simulation $N_{\mathrm{SEU,calc}}(Q_{\mathrm{fit}})$ is calculated by the following equation:

$$N_{\mathrm{SEU,calc}}(Q_{\mathrm{fit}}) = t_{\mathrm{exp}} N_{\mathrm{bit}} \int \phi_{\mathrm{facility}}(E_n)\sigma_{\mathrm{SEU}}(E_n, Q_{\mathrm{fit}})\, dE_n \quad (3)$$

where N_{bit} is the amount of SRAM bits, and ϕ_{facility} is the differential flux of the facility at which the experiment was conducted as a function of E_n.
4) *Calculation of Terrestrial SERs:* Finally, calculate the terrestrial SER SER_{GND} using the following equation:

$$\mathrm{SER}_{\mathrm{GND}} = \int \phi_{\mathrm{GND}}(E_n)\sigma_{\mathrm{SEU}}(E_n, Q_{\mathrm{fit}})\, dE_n \quad (4)$$

where ϕ_{GND} is the differential flux at the ground as a function of E_n.

III. Experimental Setup

A. Estimation Setup

We use 12-nm FinFET and 28-nm planar SRAM chips for the evaluation, which are the same as those used in [2]. The configuration of the 12-nm SRAM board for the simulation is shown in Fig. 1, and the configuration of the 28-nm SRAM board is shown in Fig. 2. The thickness parameters of some layers are often confidential; however, reference information can be found, for example, in [10] and [11]. The 12-nm FinFET SRAM chip has four types of cells: 1-fin L/S and 2-fin L/S, where L/S stands for large/small cell area. Only 1-fin L cells are used in this article, and analyzing the other cell types remains as future work. The 28-nm planar SRAM chip has two types of cells: SRAM and register file (RF). The only difference between the two in the simulation configuration is cell size. The single-sensitive volume (SSV) model [12] is utilized to calculate the amount of charge collected. For the 28-nm planar SRAM, the sensitive volume (SV) is positioned around the OFF-state nMOS drain [13], with a depth of 0.5 μm. Conversely, for the 12-nm FinFET SRAM, the SV encompasses the entire OFF-state nMOS fin beneath the gate and the fin encased by shallow trench isolation (STI) under the drain, as depicted in Fig. 3. Although we reviewed various papers to allocate the SV in the FinFET SRAM, we could not find sufficient information on the SV location. Therefore, this SV geometry was determined through technology computer-aided design (TCAD) simulations with hyper environment for exploration of semiconductor simulation (HyENEXSS) [14], which assessed the collected charge by depositing a point charge of 0.5 fC at various locations supposing a 0.8-V operation. The region where the charge collection efficiency exceeds 0.4, as depicted in Fig. 4, is identified as the SV.

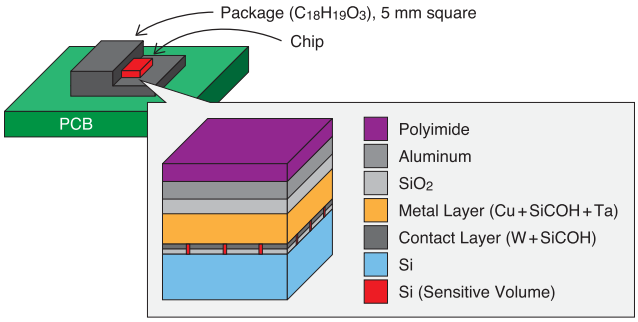

Fig. 1. Constitution of the 12-nm SRAM board in PHITS simulation.

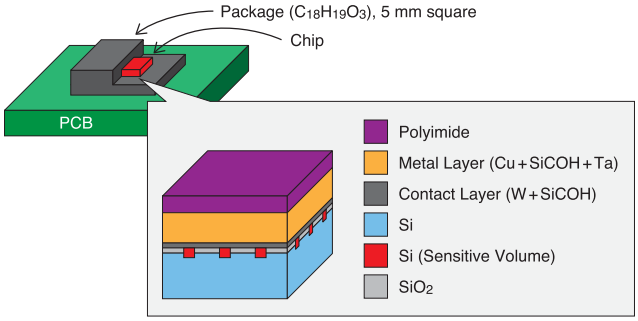

Fig. 2. Constitution of the 28-nm SRAM board in PHITS simulation.

Irradiation of monoenergetic neutrons from the package side of the DUT board is simulated by PHITS to obtain $\sigma_{\mathrm{SEU}}(E_n, Q_{\mathrm{fit}})$. The neutron energy range for the irradiation simulation spans from 0.1 to 1000 MeV, as referred to in [6]. For each neutron energy, the number of events that induce the charge whose amount is larger than Q_{fit} is evaluated from PHITS ver. 3.29 simulation with Event Generator Mode Ver. 2, which is converted into $\sigma_{\mathrm{SEU}}(E_n, Q_{\mathrm{fit}})$. Then, we determine the fitting parameter Q_{fit} and compute the terrestrial SER, following the procedure described in Section II. The terrestrial neutron energy spectrum at the ground, ϕ_{GND}, was calculated by excel-based program for calculating atmospheric cosmic-ray spectrum (EXPACS) [15], [16].

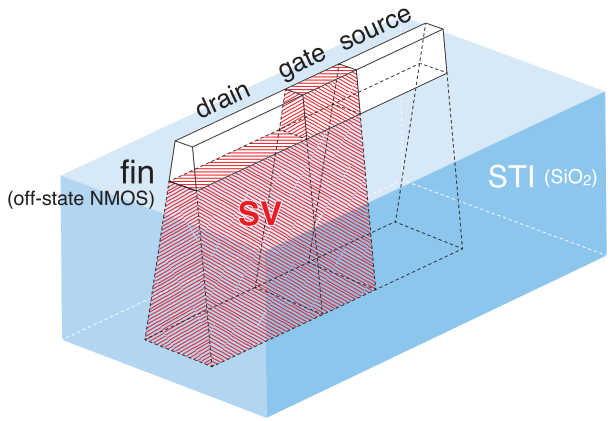

Fig. 3. Location of SV in the 12-nm FinFET SRAM for PHITS simulation.

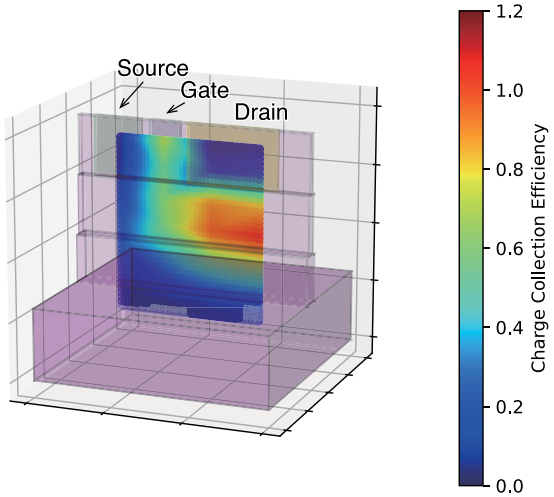

Fig. 4. Charge correction efficiency around the OFF-state nMOS transistor in the 12-nm FinFET SRAM obtained by TCAD simulation.

Figs. 5–7 present the SEU cross sections for various Q_{fit} values of 12-nm SRAM, 28-nm SRAM, and 12-nm RF, respectively. The black circles in Figs. 5–7 denote the experimental results obtained at the National Institute of Advanced Industrial Science and Technology (AIST) and the Research Center for Accelerator and Radioisotope Science (RARIS)[1] at Tohoku University [17]. All results from PHITS simulations and experiments at AIST and RARIS include error bars representing one standard deviation. The fit curves for the Weibull function are also illustrated in Figs. 5 and 6. The parameters of the Weibull function are detailed in Table I. σ_{L_i} was set to the experimental cross section at an energy of 70 MeV, and E_{0i} was determined to be 6 MeV, referring to [3].

At AIST, we repeated 30-min static tests for the 12-nm boards and 15-min tests for the 28-nm boards. All SRAM cells were preset to 1, and the operating voltage was set to 0.68 V for 12-nm boards and 0.75 V for 28-nm boards throughout the experiments. The preset value of SRAMs and the operating voltage are common through all the experiments at AIST, RARIS, and RCNP. Detailed descriptions of the DUT

[1]The former name is Cyclotron and Radioisotope Center (CYRIC).

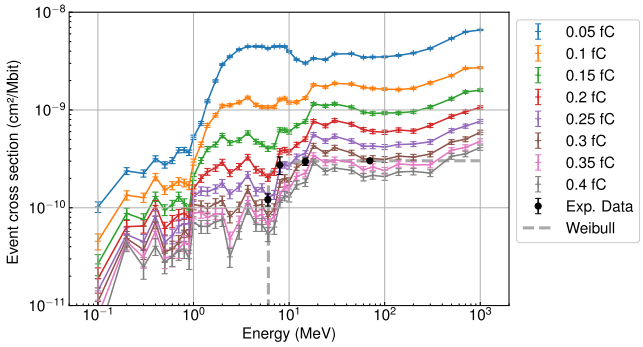

Fig. 5. SEU cross sections for various values of Q_{fit} of 12-nm SRAMs. The vertical error bar is with one standard deviation. The black circles represent the experimental results at AIST and RARIS.

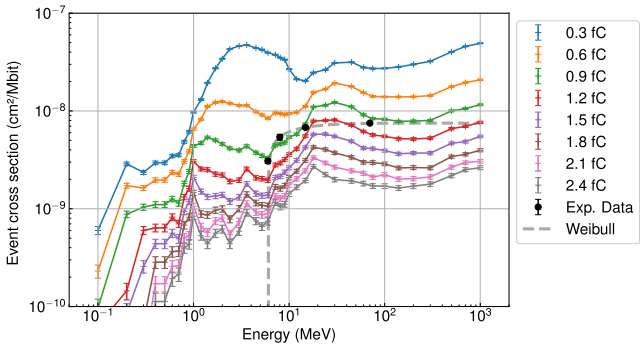

Fig. 6. SEU cross sections for various values of Q_{fit} of 28-nm SRAMs.

board configurations and the experimental setup at AIST can be found in [2]. It is important to note that although the experimental results at AIST are primarily sourced from [2], the fluence from the experiments has been reevaluated for improved precision, and the number of error events was counted separately for each SRAM cell type.

Regarding RARIS, while the same DUT boards were employed, the experimental setup was different. The DUT boards were positioned 20 cm from the beam exit, with neutrons injected from the package side. This setup underwent 12-min static tests repeatedly. The SEU cross sections at RARIS were computed using [6, eq. (2)]. The energy spectra of the quasimonoenergetic beam at RARIS are depicted in [6, Fig. 1].

To accurately calculate the SEU cross section, it is essential to distinguish multicell upsets (MCUs) from single-bit upsets (SBUs), as neutron-induced MCUs have been observed even in FinFET devices [18], [19], [20]. For the experimental data, when flipped bits are adjacent to each other, we consider them as an MCU event. For the simulation data, when more than one bit exceeds the critical charge in the same event, we classify it as an MCU.

B. Irradiation Experimental Setup for White Neutron Beams

To validate the estimation method described in [6], neutron irradiation tests were conducted on 12-nm FinFET SRAMs, 28-nm planar SRAMs, and 65-nm planar SRAMs using a white neutron beam at RCNP. These tests provided reference

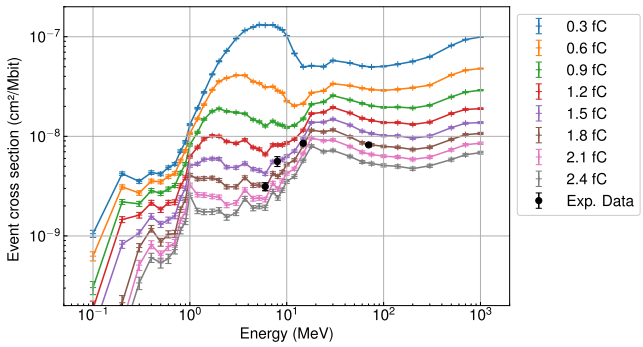

Fig. 7. SEU cross sections for various values of Q_{fit} of 28-nm RF.

TABLE I
PARAMETERS IN WEIBULL FUNCTION IN (1)

Device	σ_{L_i} (cm^2/Mbit)	W_i (MeV)	S_i (MeV)
12 nm SRAM	3.03×10^{-10}	0.169	0.354
28 nm SRAM	7.51×10^{-9}	1.12	0.415

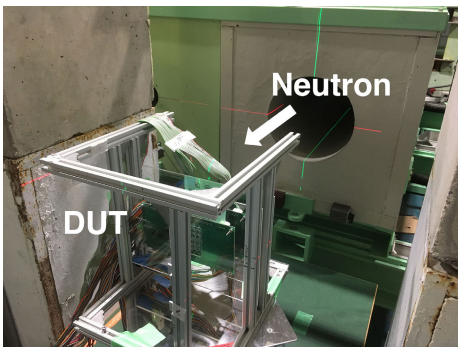

Fig. 8. Experimental setup at RCNP.

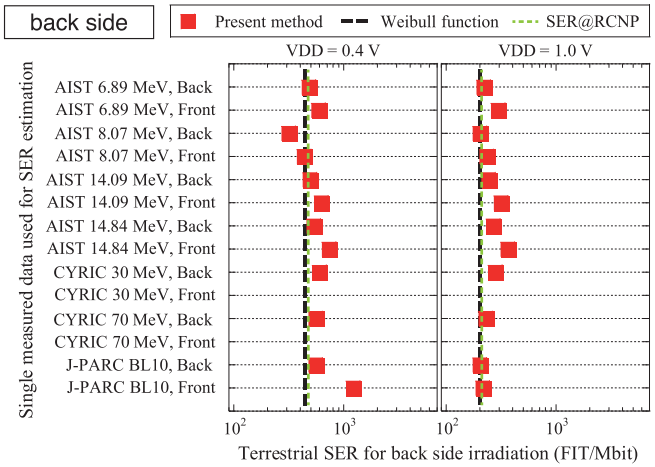

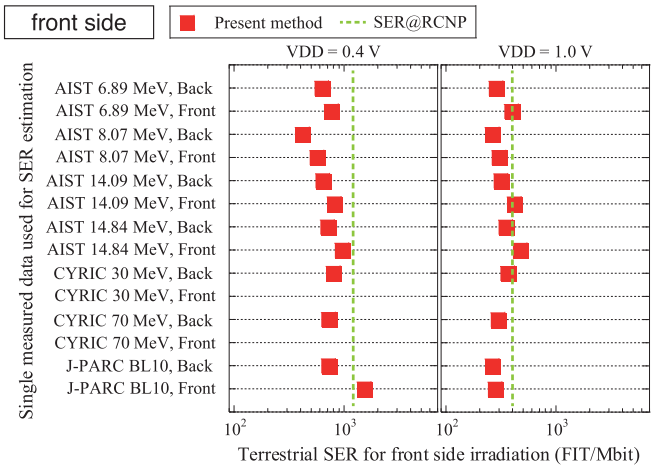

Fig. 9. Comparison of SERs estimated by Abe et al. [6] from SERs estimated by accelerating tests in 65-nm SRAMs. Vertical yellowish-green broken lines represent experimental results at RCNP. VDD indicates the operating voltage of SRAMs during hold.

SERs for evaluating accuracy. Details of the 65-nm SRAM board configuration can be found in [21]. The DUT boards were placed 80 cm away from the collimator, as depicted in Fig. 8. Neutrons were irradiated from the package side of the boards for 12- and 28-nm SRAMs, and both sides of the boards for 65-nm SRAMs. We conducted repeated 12-min static tests until over 100 error events were obtained.

We calculated the terrestrial SER for reference, $\text{SER}_{\text{GND}}^{\text{ref}}$ using (5) and the accelerating factor at RCNP, Acc_{RCNP}, given by (6)

$$\text{SER}_{\text{GND}}^{\text{ref}} = \frac{\text{SER}_{\text{RCNP}}}{\text{Acc}_{\text{RCNP}}} = \frac{N_{\text{errors}}}{t_{\text{exp}} \cdot N_{\text{bit}} \cdot \text{Acc}_{\text{RCNP}}} \tag{5}$$

$$\text{Acc}_{\text{RCNP}} = \frac{\int_{E_{\text{min}}}^{\infty} \phi_{\text{RCNP}}(E_n)\, dE_n}{\int_{E_{\text{min}}}^{\infty} \phi_{\text{GND}}(E_n)\, dE_n}. \tag{6}$$

The minimum energy of neutrons considered in the acceleration factor at RCNP, E_{min}, was set to 0.1 MeV to align with the energy range of neutrons used in the computation of SER_{GND} in (4). Note that E_{min} of 10 MeV found in JESD89B [1] is not appropriate here since the SEU cross section is not negligibly small compared with that of >10 MeV.

IV. RESULTS AND DISCUSSION

A. Experimental Results for 65-nm SRAMs

We calculated $\text{SER}_{\text{GND}}^{\text{ref}}$ for 65 nm using (5). Fig. 9 shows the experimental results at RCNP. The SERs estimated by the SER estimation method in [6] were extracted from [6]. The "back" side represents estimated SERs when the chips are irradiated from PCB sides, and the "front" side represents ones when the chips are irradiated from package sides. Since the package of the chip can generate secondary H ions due to abundant hydrogen atoms in the package material, there is a difference between the SER for the front side and that for the back side as described in [6].

For the back side, the maximum absolute errors between the experimental results at RCNP and the estimated SERs are 156% for 0.4 V and 70% for 1.0 V. If the SER estimated by "J-PARC BL10, Front" is excluded, they are 55% for 0.4 V. In addition, the ratio of the measured SER at RCNP to the calculated SER by the Weibull function is 1.07 for 0.4 V and 1.04 for 1.0 V for the back side.

For the front side, the maximum absolute errors between the experimental results at RCNP and the estimated SERs are

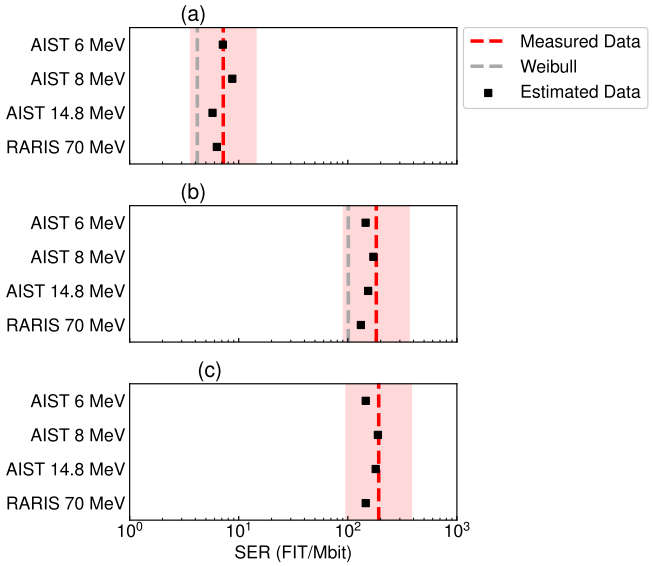

Fig. 10. Comparison of SERs estimated by Abe et al. [6] from SERs estimated by accelerating tests in 12- and 28-nm SRAMs and a 28-nm RF. Red broken lines represent experimental results at RCNP, and the black squares correspond to SER estimation results. Pale red backgrounds show the ranges between 50% of test results and double ones. (a) 12-nm SRAM at 0.68 V. (b) 28-nm SRAM at 0.75 V. (c) 28-nm RF at 0.75 V.

66% for 0.4 V and 35% for 1.0 V. Here, due to the insufficient number of experimental data at quasimonoenergetic neutron sources, the SER estimated by the Weibull function is not included in Fig. 9 for the front side. In contrast with the back side, almost all the estimated SERs by Abe et al. [6] are lower than the results at RCNP for 0.4 V.

B. Experimental and Estimated Results for 12- and 28-nm SRAMs

We estimated terrestrial SERs $\mathrm{SER_{GND}}$ using the evaluation method described in Section II and [6], based on the measured data of 14.8-, 8-, 6-, and 70-MeV quasimonoenergetic neutrons. It is important to note that each SER estimate utilizes the result from a single-neutron source. Fig. 10 shows the results of accelerated tests and SER estimations. The estimated SERs, along with the Weibull fitting, are also illustrated in Fig. 10 for comparison. The maximum absolute differences between the experimental results at RCNP and the estimated SERs are 21% for the 12-nm SRAM, 28% for the 28-nm SRAM, and 24% for the 28-nm RF. Furthermore, the ratio of the maximum estimated values to the minimum ones is 1.52 for the 12-nm SRAM, 1.30 for the 28-nm SRAM, and 1.29 for the 28-nm RF. These outcomes indicate that the estimation method described in [6] is valuable for future use.

Meanwhile, the SERs estimated with the Weibull function are found to be underestimated for both types of SRAMs. This discrepancy is believed to stem from differences in the SEU cross sections below 6 MeV, as observed between the PHITS simulations and the Weibull function estimations. Given that Abe et al. [22] have indicated hydride materials near the transistors can impact the SEU cross section at energies of several MeV, reliance on the original Weibull function for SER estimation may not yield the expected accuracy.

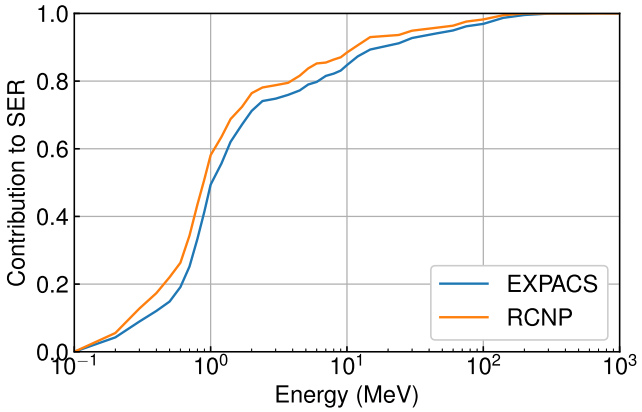

Fig. 11. Cumulative plots of the contribution to the 12-nm SRAM SER at 0.68 V as a function of neutron energy. The blue line indicates the results obtained from the terrestrial spectrum, and the orange line shows the results obtained from the RCNP spectrum.

C. Discussion

So far, the SER obtained from the RCNP irradiation test and its acceleration factor is regarded as a golden reference. However, the energy spectrum of RCNP does not perfectly match that of the terrestrial environment. Fig. 11 shows cumulative plots of the contribution to the 12-nm SRAM SER at 0.68 V as a function of neutron energy, comparing the RCNP spectrum with the terrestrial spectrum. A clear difference is observed in the low-energy range of less than 1 MeV. Due to the larger portion of low-energy neutrons at RCNP, SEUs induced by low-energy neutrons are expected to be counted more frequently at RCNP than in the terrestrial environment.

We applied the cross section of the 12-nm SRAM obtained by PHITS with $Q_{\mathrm{fit}} = 0.39$ fC for both the RCNP and terrestrial energy spectra and computed the SERs. The SER for the RCNP spectrum is 4.94 FIT/Mb, while that for the terrestrial spectrum is 7.15 FIT/Mb, indicating a 45% difference. Considering this uncertainty of 45%, the difference between the measured SERs at RCNP and the estimated SERs, as discussed in Sections IV-A and IV-B, is not a significant issue.

V. Influence of Dielectric Material in Metal Layers

In advanced technologies, low-k materials, such as SiCOH, are used as dielectric materials in metal layers for the reduction of parasitic capacitance [23]. Following this trend, in the previous section, we adopted SiCOH instead of SiO_2 on PHITS simulation (so-called SiCOH model) for 12- and 28-nm devices. Also, Ta, used as a barrier metal, was embedded into the simulation configuration. However, it is usually difficult to obtain the details of materials in chips since semiconductor chip fabricators rarely disclose their secrets. Consequently, missing material information could affect soft error simulation and SER estimation.

To assess the impact of dielectric materials, we replaced SiCOH with SiO_2 in the existing PHITS simulation configuration (so-called SiO_2 model), where SiO_2 had been used as the dielectric material for a long time. Additionally, Ta was

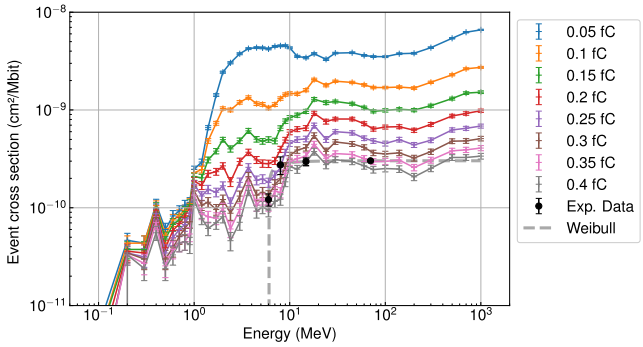

Fig. 12. SEU cross sections for various values of Q_{fit} of 12-nm SRAMs (SiO_2 model). The vertical error bar is with one standard deviation. The black circles represent the experimental results at AIST and RARIS.

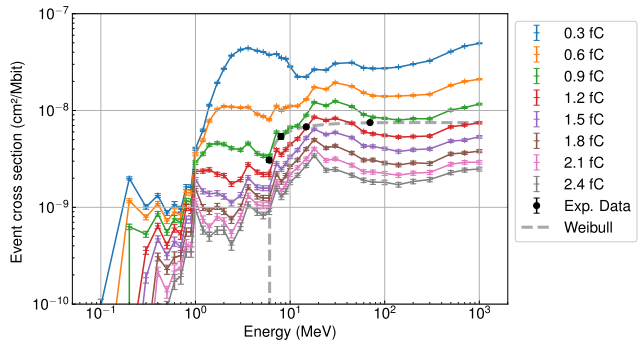

Fig. 13. SEU cross sections for various values of Q_{fit} of 28-nm SRAMs (SiO_2 model).

removed from the simulation constitution. Figs. 12 and 13 show the SEU cross sections for various Q_{fit} values of 12- and 28-nm SRAMs with SiO_2, respectively. The black circles and gray broken lines are the same as Figs. 5 and 6.

We estimated terrestrial SERs in the same way as Section IV, using the simulation configuration with SiO_2 as dielectric materials. Fig. 14 shows the results of accelerated tests and SER estimations. The measured data at RCNP and the estimated data by the Weibull function are the same as Fig. 10. The maximum absolute differences between the experimental results at RCNP and the estimated SERs are 50% for 12-nm SRAMs and 34% for 28-nm SRAMs. For both 12- and 28-nm SRAMs, the estimated SERs from the measured data of AIST 14.8 MeV are the worst in terms of accuracy. In addition, the ratio of the maximum estimated values to the minimum ones is 2.38 for 12-nm SRAMs and 1.32 for 28-nm SRAMs, which are larger than those discussed in the previous section with the SiCOH model.

It is considered that this outcome originates from the difference between the SEU cross sections at high energies and ones at low energies (see Figs. 5 and 12 for the 12-nm SRAM, and Figs. 6 and 13). For instance, in the 12-nm SRAM, the ratio of the SEU cross section at 14.8 MeV to that at 8 MeV is 1.65 for the SiCOH simulation model with 0.3 fC. However, for the SiO_2 simulation model with 0.4 fC, the ratio is 2.39. This significant drop in the SEU cross section for the SiO_2 model leads to the underestimation of terrestrial SERs.

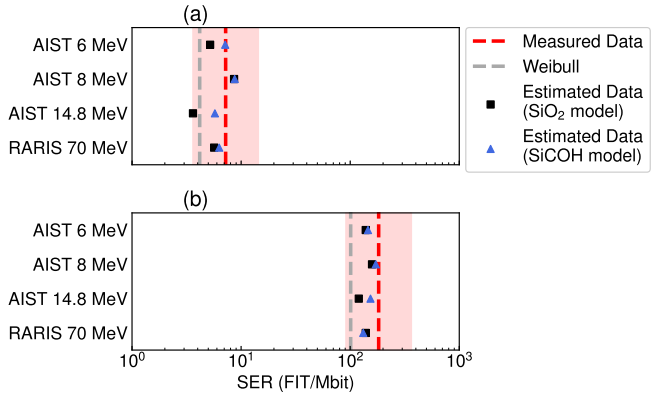

Fig. 14. Comparison of SERs estimated by Abe et al. [6] from SERs estimated by accelerating tests, using the SiO_2 model. Red broken lines represent experimental results at RCNP, and the black squares correspond to SER estimation results. Pale red backgrounds show the ranges between 50% of test results and double ones. Estimated data (SiCOH model) are the same as Fig. 10. (a) 12-nm SRAM at 0.68 V. (b) 28-nm SRAM at 0.75 V.

As mentioned in Section IV, hydride materials near the SV contribute to the SEU cross section for low-energy (<10 MeV) neutrons [22], which explains the underestimation of the SEU cross section in the SiO_2 model. Furthermore, compared with the SiCOH model, the SEU cross sections for the SiO_2 model with 0.4 fC at around 100 MeV are smaller than those at 14.8 MeV.

On the other hand, the estimated terrestrial SERs from the other measured data do not show a significant difference compared to those obtained with the SiCOH model. It is believed that because the AIST 6 and 8 MeV and RARIS 70-MeV sources contain many low-energy neutrons, the estimated SERs from these data are rarely affected.

The discussion above indicates that modeling hydride materials near the SV is important for improving the accuracy of SER estimation, whereas differences in dielectric materials do not introduce critical errors. Since dielectric materials change with advancing technology, it is crucial to monitor these changes carefully and incorporate them into simulations performed with Monte Carlo radiation transport codes.

VI. Conclusion

The SERs for 12- and 28-nm SRAMs were estimated through simulations combined with a one-time irradiation experiment. The estimation method proposed by Abe et al. produced acceptable terrestrial SERs with a deviation of up to 28% across two SRAM fabrication technologies and various facilities where the irradiation tests were conducted. This outcome indicates that the method applies to both planar and FinFET SRAMs. In addition, the SERs for 65-nm SRAMs were measured using a white neutron source. The absolute errors between the experimental results at RCNP and the estimated SERs by Abe et al. [6] are up to 70% for 1.0 V.

The influence of dielectric materials on SER estimation was also evaluated. The accuracy of SER estimation deteriorated by up to 26%, highlighting that modeling hydride materials near the SV in Monte Carlo simulations improves accuracy. On the other hand, this result does not undermine the value of the method in [6]. The method in [6] provides results equivalent

to existing SER evaluation standards in terms of accuracy, regardless of the dielectric materials.

ACKNOWLEDGMENT

The authors appreciate Dr. Kato from Socionext Inc., and Kozo Takeuchi from JAXA for their valuable discussions. The work cooperated with the Association for Quantum Beam Applications for Safe and Smart Society (QASS).

REFERENCES

[1] *Measurement and Reporting of Alpha Particle and Terrestrial Cosmic Ray-Induced Soft Errors in Semiconductor Devices*, Standard JEDEC JESD89B, 2021.

[2] K. Takami et al., "Characterizing SEU cross sections of 12- and 28-nm SRAMs for 6.0, 8.0, and 14.8 MeV neutrons," in *Proc. IEEE Int. Rel. Phys. Symp. (IRPS)*, Mar. 2023, pp. 728–733, doi: 10.1109/IRPS48203.2023.10118134.

[3] W. Liao, K. Ito, S.-I. Abe, Y. Mitsuyama, and M. Hashimoto, "Characterizing energetic dependence of low-energy neutron-induced SEU and MCU and its influence on estimation of terrestrial SER in 65-nm bulk SRAM," *IEEE Trans. Nucl. Sci.*, vol. 68, no. 6, pp. 1228–1234, Jun. 2021, doi: 10.1109/TNS.2021.3077266.

[4] H. Quinn, A. Watkins, L. Dominik, and C. Slayman, "The effect of 1–10-MeV neutrons on the JESD89 test standard," *IEEE Trans. Nucl. Sci.*, vol. 66, no. 1, pp. 140–147, Jan. 2019, doi: 10.1109/TNS.2018.2884908.

[5] C. Qi et al., "Influence of 0.1–10 MeV neutron-induced SEUs on estimation of terrestrial SER in a nano-scale SRAM," *AIP Adv.*, vol. 13, no. 11, Nov. 2023, Art. no. 115207, doi: 10.1063/5.0174117.

[6] S.-I. Abe et al., "A terrestrial SER estimation methodology based on simulation coupled with one-time neutron irradiation testing," *IEEE Trans. Nucl. Sci.*, vol. 70, no. 8, pp. 1652–1657, Aug. 2023, doi: 10.1109/TNS.2023.3280190.

[7] T. Sato et al., "Recent improvements of the particle and heavy ion transport code system—PHITS version 3.33," *J. Nucl. Sci. Technol.*, vol. 61, no. 1, pp. 127–135, 2024, doi: 10.1080/00223131.2023.2275736.

[8] S. Agostinelli, "GEANT4—A simulation toolkit," *Nucl. Instrum. Methods Phys. Res. A, Accel. Spectrom. Detect. Assoc. Equip.*, vol. 506, no. 3, pp. 250–303, 2003, doi: 10.1016/S0168-9002(03)01368-8.

[9] Y. Iwamoto et al., "Evaluation of the white neutron beam spectrum for single-event effects testing at the RCNP cyclotron facility," *Nucl. Technol.*, vol. 173, no. 2, pp. 210–217, Feb. 2011, doi: 10.13182/nt11-a11550.

[10] S.-Y. Wu et al., "A 16nm FinFET CMOS technology for mobile SoC and computing applications," in *IEDM Tech. Dig.*, Washington, DC, USA, Dec. 2013, pp. 224–227, doi: 10.1109/IEDM.2013.6724591.

[11] L. Collins. *TSMC 16 nm FinFET, Ge 20 nm P-FinFET Set for IEDM*. Tech Design Forum. Accessed: Nov. 26, 2024. [Online]. Available: https://www.techdesignforums.com/blog/2013/10/01/tsmc-16nm-finfet-ge-20nm-p-finfet-set-iedm/

[12] E. L. Petersen, J. C. Pickel, E. C. Smith, P. J. Rudeck, and J. R. Letaw, "Geometrical factors in SEE rate calculations," *IEEE Trans. Nucl. Sci.*, vol. 40, no. 6, pp. 1888–1909, Dec. 1993, doi: 10.1109/23.273465.

[13] P. Roche, J. M. Palau, G. Bruguier, C. Tavernier, R. Ecoffet, and J. Gasiot, "Determination of key parameters for SEU occurrence using 3-D full cell SRAM simulations," *IEEE Trans. Nucl. Sci.*, vol. 46, no. 6, pp. 1354–1362, Dec. 1999, doi: 10.1109/23.819093.

[14] N. Kotani, "TCAD in selete," in *Proc. Int. Conf. Simulation Semiconductor Processes Devices (SISPAD)*, 1998, Paper 3-D.

[15] T. Sato, "Analytical model for estimating the zenith angle dependence of terrestrial cosmic ray fluxes," *PLoS ONE*, vol. 11, no. 8, Aug. 2016, Art. no. e0160390, doi: 10.1371/journal.pone.0160390.

[16] T. Sato, "Analytical model for estimating terrestrial cosmic ray fluxes nearly anytime and anywhere in the world: Extension of PARMA/EXPACS," *PLoS ONE*, vol. 10, no. 12, Dec. 2015, Art. no. e0144679, doi: 10.1371/journal.pone.0144679.

[17] Y. Sakemi, M. Itoh, and T. Wakui, "High intensity fast neutron beam facility at CYRIC," in *Proc. Int. Atomic Energy Agency (IAEA)*, Vienna, Austria, Jul. 2014, pp. 229–233.

[18] Y.-P. Fang and A. S. Oates, "Characterization of single bit and multiple cell soft error events in planar and FinFET SRAMs," *IEEE Trans. Device Mater. Rel.*, vol. 16, no. 2, pp. 132–137, Jun. 2016, doi: 10.1109/TDMR.2016.2535663.

[19] T. Kato, M. Hashimoto, and H. Matsuyama, "Angular sensitivity of neutron-induced single-event upsets in 12-nm FinFET SRAMs with comparison to 20-nm planar SRAMs," *IEEE Trans. Nucl. Sci.*, vol. 67, no. 7, pp. 1485–1493, Jul. 2020, doi: 10.1109/TNS.2020.2989446.

[20] N. J. Pieper et al., "Study of multicell upsets in SRAM at a 5-nm bulk FinFET node," *IEEE Trans. Nucl. Sci.*, vol. 70, no. 4, pp. 401–409, Apr. 2023, doi: 10.1109/TNS.2023.3240318.

[21] W. Liao, K. Ito, Y. Mitsuyama, and M. Hashimoto, "Characterizing energetic dependence of low-energy neutron-induced MCUs in 65 nm bulk SRAMs," in *Proc. IEEE Int. Rel. Phys. Symp. (IRPS)*, Apr. 2020, pp. 657–661, doi: 10.1109/IRPS45951.2020.9129621.

[22] S.-I. Abe et al., "Impact of hydrided and non-hydrided materials near transistors on neutron-induced single event upsets," in *Proc. IEEE Int. Rel. Phys. Symp. (IRPS)*, Apr. 2020, pp. 630–635, doi: 10.1109/IRPS45951.2020.9128951.

[23] *International Roadmap for Devices and Systems 2016 Edition More Moore White Paper*, IEEE, Piscataway, NJ, USA, 2016.